

# Dynamics of Mars Trojans

H. Scholl <sup>a,\*</sup>, F. Marzari <sup>b</sup>, P. Tricarico <sup>c</sup>

<sup>a</sup> *Observatoire de la Côte d'Azur, Nice, France*

<sup>b</sup> *Dipartimento di Fisica, Università di Padova, 35131 Padova, Italy*

<sup>c</sup> *Department of Physics, Washington State University, Pullman, WA 99164, USA*

Received 21 September 2004; revised 23 December 2004

Available online 24 March 2005

## Abstract

In this paper we explore the dynamical stability of the Mars Trojan region applying mainly Laskar's Frequency Map Analysis. This method yields the chaotic diffusion rate of orbits and allows to determine the most stable regions. It also gives the frequencies which are responsible for the instability of orbits. The most stable regions are found for inclinations between about 15° and 30°. For inclinations smaller than 15°, we confirm, by applying a synthetic secular theory, that the secular resonances  $\nu_3$ ,  $\nu_4$ ,  $\nu_{13}$ ,  $\nu_{14}$  rapidly excite asteroid orbits within a few Myrs, or even faster. The asteroids are removed from the Trojan region after a close encounter with Mars. For large inclinations, the secular resonance  $\nu_5$  clears a small region around 30° while the Kozai resonance rapidly removes bodies for inclinations larger than 35°. The dynamical lifetimes of the three L5 Trojans, (5261) Eureka, 1998 VF31, 2001 DH47, and the only L4 Trojan 1999 UJ7 are determined by numerically integrating clouds of corresponding clones over the age of the Solar System. All four Trojans reside in the most stable region with smallest diffusion coefficients. Their dynamical half-lifetime is of the order of the age of the Solar System. The Yarkovsky force has little effect on the known Trojans but for bodies smaller than about 1–5 m the drag is strong enough to destabilize Trojans on a timescale shorter than 4.5 Gyr.

© 2005 Elsevier Inc. All rights reserved.

*Keywords:* Asteroids; Mars Trojans

## 1. Introduction

According to Lagrange's solution of the three-body problem, any planet in the Solar System might harbor asteroids in Trojan type orbits librating around the respective Lagrangian points L4 or L5. However, secular frequencies of the planetary system may destabilize on the long term these orbits removing its possible primordial Trojan population totally or reducing it to a small number of objects. Planetary migration may also alter a primordial Trojan population, in particular when a planet crosses a mean motion resonance with another planet or if the migration rate of a planet is too large. It is also possible that a planet may capture Trojans during migration (Morbiddelli et al., 2004). Hence, Trojans

did not necessarily form around the Lagrangian points of a planet. The Jupiter Trojan population is the largest known with more than 1000 recorded members. There is a striking majority of Jupiter Trojans librating around the leading Lagrangian point L4. It is not yet clear if this is an observational effect which favored the discovery of L4 Trojans. In the frame of the purely gravitational problem including all planets, no asymmetry is known between the L4 and L5 region. There is, on the other hand, an asymmetry in the presence of a drag-like effect as, for instance, gas drag (Peale, 1993; Marzari and Scholl, 1998; Murray, 1994). The asymmetry is due to the eccentricity of Jupiter's orbit which aligns the perihelia of Trojans at an angle of 270° with respect to Jupiter's perihelion. One Neptune Trojan, 2001 QR322, was found in the Lowell Observatory's Deep Ecliptic Survey team (Millis et al., 2002) to librate around L4 (Marzari et al., 2003b; Brassier et al., 2004). Since the size of the stable region of Neptune Trojans is comparable to Jupiter's region, the Nep-

\* Corresponding author. Fax: +33-492003121.  
E-mail address: [scholl@obs-nice.fr](mailto:scholl@obs-nice.fr) (H. Scholl).

tune Trojan region appears to be clearly underpopulated, presumably due to a cosmogonic reason. No Trojan is known for Uranus neither for Saturn. The Trojan regions of both are less stable as compared to Jupiter and Neptune (Nesvorny and Dones, 2002; Marzari et al., 2002, 2003a, 2003b). In the case of Mars, the three Trojans (5261) Eureka, 1998 VF31, and 2001 DH47 are known to librate around the trailing Lagrangian point L5. One Trojan, 1999 UJ7, resides in the L4 region. All four Mars Trojans have a comparatively small size with a diameter of the order of 1 km. Diameters for Eureka and 1998 VF31 were derived by Rivkin et al. (2003). Since the other two Trojans have similar magnitudes, their sizes can be expected to be of the same order. Rivkin et al. (2003) determined the spectral classes of three Mars Trojans, the two L5 Trojans Eureka and 1998 VF31, and of the only known L4 Trojan 1999 UJ7. The latter Trojan has a X-class or T-class spectrum with a wide range of possible meteorite analogies. The two L5 Trojans belong to the very rare Sr or A class. This means that they might have been part of a larger differentiated parent body which suffered disruption.

What is the origin of the Mars Trojans? They might be primordial bodies which formed in the Trojan region, or they may have been captured in an early phase of the Solar System at the end of the migration of Mars as suggested by Morbidelli et al. (2004) or they may have entered the Trojan region much later. A disruption of the parent body of Eureka and 1998 VF31 in the Trojan region is quite unlikely due to the very different orbital inclinations of about 20° and 31°, respectively. Another question is whether or not the known Trojans fill most of the region which is stable over the age of the Solar System or if, like in the case of Neptune, the stable regions are clearly underpopulated.

In this paper we estimate the dynamical lifetimes of the four known Mars Trojans and we explore in detail the stability of the regions around the Lagrangian points. Since the known Mars Trojans are km-sized objects, their orbital evolution and stability is subjected to the Yarkovsky effect (see Bottke et al. (2002) for a review) which might destabilize their orbits. The strength of the Yarkovsky force depends on various physical properties of an asteroid, in particular on its size. One can expect a critical minimum size for asteroids to resist against the Yarkovsky effect in the Mars Trojan region. Smaller asteroids would be removed. We present here results of long-term integrations of Mars Trojan orbits under the effect of the Yarkovsky force.

Several authors investigated in the past the stability of Mars Trojans (Mikkola and Innanen, 1994; Tabachnik and Evans, 1999, 2000) over a maximum timescale of 100 Myr. It was found that low inclined and very high inclined orbits are rapidly destabilized. Stable orbits over a timescale of 100 Myr have inclinations between about 15° and 35°. The instability of low inclined orbits was attributed by Brassier and Lehto (2002) to the secular resonances  $\nu_3$ ,  $\nu_4$ ,  $\nu_{13}$ , and  $\nu_{14}$  while the destabilizing mechanism at high inclination was unknown. We extended the stability analysis over timescales of the age of the Solar System by exploring the

whole phase space of the Mars Trojan region combining Laskar's (Laskar et al., 1992; Laskar, 1993a, 1993b) Frequency Map Analysis (hereinafter FMA) with long-term numerical integrations of selected orbits. For the determination of the dynamical lifetimes of the four Mars Trojans, we integrated a cloud of 20 clones of each Trojan which yields an estimation for their dynamical half-lifetimes. We also computed the Lyapunov time which is a classical indicator for chaos.

The application of the FMA method, which provides a measure for the chaotic diffusion of orbits, yields also the proper frequencies of orbits as a function of proper elements. We develop a secular theory for Trojans which gives the secular resonances responsible for the chaotic diffusion and for the instability of orbits.

## 2. Search for the most stable regions

We integrate the motion of a large number of test bodies in Trojan type orbits and measure their chaotic diffusion by the FMA method (Laskar et al., 1992; Laskar, 1993a, 1993b). The idea of the FMA method is to determine the diffusion rate of the proper frequencies which appear in the spectra of orbital elements. The diffusion rate is a measure for the stability of an orbit. Spectra are obtained on running time windows. The advantage of this method is the comparatively short time interval for a numerical integration which is necessary to obtain the diffusion rate for an orbit. In the case of Mars Trojans, integrations over 10 Myr are sufficient to obtain reliable diffusion rates. This makes the FMA method a very attractive method to explore the phase space and is much faster than the computation of Lyapunov times which requires much longer integration periods. In addition, the FMA yields the proper frequencies of the systems which, compared with the fundamental frequencies of the Solar System, allow to determine resonances involved in the chaotic diffusion. The resulting lowest diffusion rates indicate the most stable regions. The method gives only relative timescales for diffusion and, hence, for stability. In order to calibrate the results with absolute time in yrs, numerical integrations of orbits representing selected diffusion rates are necessary over timescales of Gyrs. In this way, dynamical lifetimes of bodies in years are obtained in regions with different diffusion rates.

### 2.1. Numerical methods

Before applying the FMA method, we sample orbits which are stable over 10 Myr in a model including all planets except Pluto. We choose orbital elements at random. Inclinations vary from 0° to 50° and eccentricities are selected between 0 and 0.3. The semimajor axes range from 0.98 to 1.02 times the semimajor axis of Mars. We include both L4 and L5 Trojan orbits and no significant asymmetry was found

between the two clouds. Orbits are integrated by the classical WHM integrator (Wisdom and Holman, 1991) which is part of the SWIFT package (Levison and Duncan, 1994). A timestep of 5 days is used and the solution for planet Mercury obtained with the WHM integrator was tested against the solution given by the RADAU (Everhart, 1985) integrator. Orbits which are stable over 10 Myr are digitally filtered with a procedure described in detail in Carpino et al. (1987). We apply a low-pass digital filter that removes all short periodic terms with frequencies higher than the libration frequency of Mars Trojans. The minimum libration period in our sample of stable orbits is 1200 years while the dark band covers periods up to about 800 years.

The filtered database of Trojan orbits is analyzed with the FMA method to measure the rate of the chaotic diffusion. The numerical algorithm is available as part of the ORSA framework (<http://orsa.sourceforge.net>). It performs a detailed spectral analysis of the complex signal  $h + ik$  with the non-singular variables  $h$  and  $k$  defined by  $h = e \cos(\varpi)$  and  $k = e \sin(\varpi)$  (Šidlichovský and Nesvorný, 1997; Nesvorný and Ferraz-Mello, 1997; Melita and Brunini, 2001; Marzari et al., 2002). The proper frequency  $g$  is computed over running windows covering the whole timespan of the numerical integration. Each window is 3 Myr wide and it is moved along the time axis for 1.5 Myr. The choice of the running window time span was motivated by the period  $T = 1/g$  of some high inclination Trojan orbits which can be as long as 1.5 Myr. Proper elements  $e_p$  and  $i_p$  are computed for each orbit from the amplitude of the proper frequency  $g$  and  $s$  in the power spectrum computed in the first window. To derive

$s$  we perform the spectral analysis of the  $p$  and  $q$  variables. The proper libration amplitude  $D$  is estimated as mean of the maximum libration amplitude computed over running windows of  $1 \times 10^5$  years over the first  $3 \times 10^6$  years of our 10 Myr numerical integration. This method was tested in Marzari et al. (2002) for Jupiter Trojans and it gave reliable results. The diffusion rate is estimated as the negative logarithm of the standard deviation  $s_g$  of the frequencies  $g$  calculated on all the windows by:  $\sigma = -\log_{10}(s_g/g)$ .

## 2.2. Diffusion maps

The diffusion rate depends on three major parameters, namely, the proper elements  $e_p, i_p$ , and the libration amplitude  $D$ . The presentation of rates as a function of these parameters is called a diffusion map. Due to practical reasons, we present here only 2D diffusion maps selecting sections by keeping, for instance, the inclination fixed or using a projection of the full map on a plane defined, for instance, by  $e_p$  and  $i_p$ . The first map shown in Fig. 1 is generated by plotting the diffusion rate of about 8000 orbits as a function of  $e_p$  and  $i_p$ . Blue color (dark) means fast diffusion while red (light) refers to slow diffusion. The white areas mean that we could not make an FMA analysis since the corresponding orbits destabilized rapidly before 10 Myr. There is in particular a white stripe at inclinations of  $i_p \sim 28^\circ - 30^\circ$ . This is due to the secular resonance  $\nu_5$  which destabilizes rapidly orbits. Slow diffusion occurs in a region extending from  $i_p \sim 13^\circ$  to  $i_p \sim 28^\circ$  for eccentricities below 0.15. The typical value of  $\sigma$  in this region lies between 2.5 and 3.0. This is the most

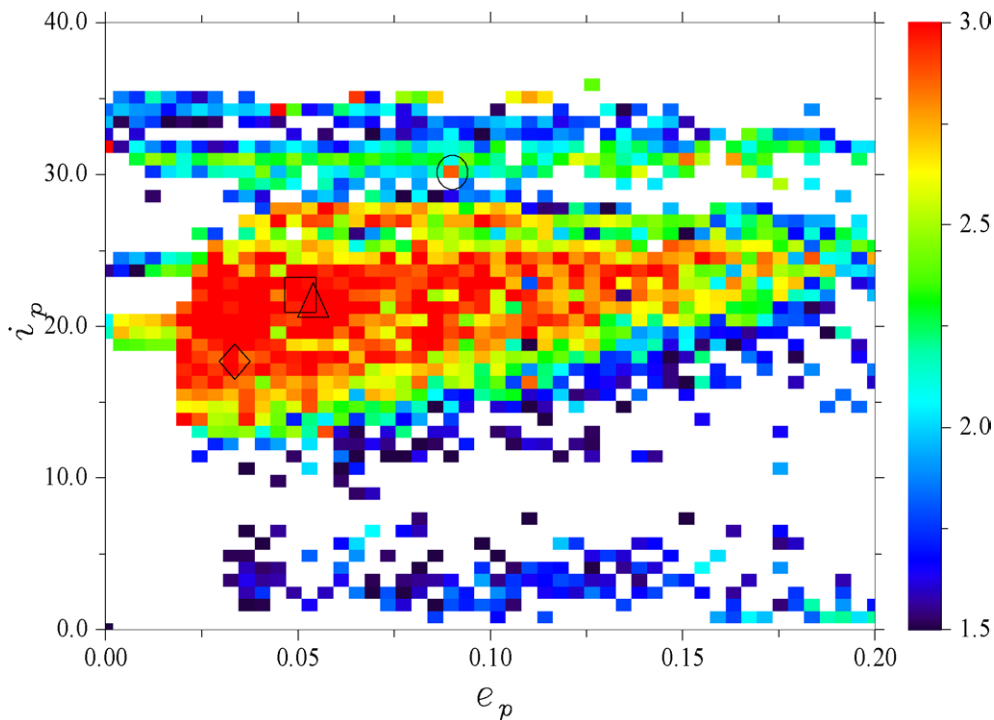


Fig. 1. Diffusion map of Mars Trojans in the  $e_p, i_p$  plane. The color scale measures the diffusion rate ( $\sigma$ ). The three Trojans Eureka (triangle), 1999 UJ7 (square), and 2001 DH47 (rhombus) reside well in its center while 1998 VF31 (empty circle) is on a stable island.

stable region. The three Trojans Eureka (triangle), 1999 UJ7 (square), and 2001 DH47 (rhombus) reside well in its center while 1998 VF31 (empty circle) is on a stable island above the unstable stripe due to the secular resonance  $\nu_5$ . Table 1 shows orbital parameters of the four Trojans.

In order to explore the chaotic diffusion as a function of libration amplitude  $D$ , we present diffusion maps in the  $e_p$  vs  $D$  space for thin slices in proper inclination, defined by a fixed value of  $i_p$  and a  $\pm 2.5^\circ$  tolerance. Three thin slices are selected for proper inclinations  $i_p = 15^\circ \pm 2.5^\circ$  (Fig. 2),  $i_p = 20^\circ \pm 2.5^\circ$  (Fig. 3), and  $i_p = 25^\circ \pm 2.5^\circ$  (Fig. 4). It is interesting to note that the region of stable orbits extend to large libration amplitudes up to  $D \sim 150^\circ$ . Trojans can get to a short angular distance from the planet without being destabilized. The higher proper eccentricity for a stable Mars Trojan orbit appears to be about 0.2 when the inclination is around  $25^\circ$ . It is a quite unexpected result that the stable region is apparently cut at very small proper eccen-

tricity, lower than  $\sim 0.02$ . These features might be important for observational strategies to discover more Trojans.

Our results confirm and extend the results of Mikkola and Innanen (1994) and Tabachnik and Evans (1999, 2000). They found with short term integrations (4.5 Myr for Mikkola and Innanen; 100 Myr for Tabachnik and Evans) that Mars Trojan orbits are stable only within the inclination windows  $15^\circ < i_0 < 30^\circ$  and  $32^\circ < i_0 < 44^\circ$  where  $i_0$  is the initial inclination, always higher than the proper inclination  $i_p$ .

At this stage we still have to answer the two questions: (1) Which resonances destabilize Mars Trojans at low and high inclinations? (2) What is the dynamical lifetime of Trojans in the most stable region?

The next sections are devoted to answer these two questions.

### 3. Synthetic secular theory

Since the chaotic orbits are destabilized on longer time-scales it is natural to assume secular resonances as the major cause for chaos and instability. A fully reliable way to determine the location of secular resonances is to develop a synthetic secular theory predicting the proper frequencies as a function of the proper elements. The idea of developing a secular theory by means of numerical procedures has been already used for Jupiter, Saturn, Uranus, and Neptune Trojans (Milani, 1994; Marzari et al., 2002, 2003a, 2003b). Once extracted the proper elements and the proper frequencies with the FMA analysis of the numerical database, we

Table 1  
Physical properties of the known Mars Trojans

Trojan	L	Ecc	Incl	Amp	Spc	Diam
Eureka	L5	0.06	20.3°	8°	Sr/A	1.2 km
1998 VF31	L5	0.10	31.3°	50°	Sr/A	0.65 km
2001 DH47	L5	0.03	24.3°	80°	–	–
1999 UJ7	L4	0.04	16.8°	75°	X/T	–

L refers to the Lagrangian point, Ecc and Incl are the present osculating eccentricity and inclination, respectively, Amp is the present libration amplitude, Spc and Diam are the spectral class and diameter according to Rivkin et al. (2003).

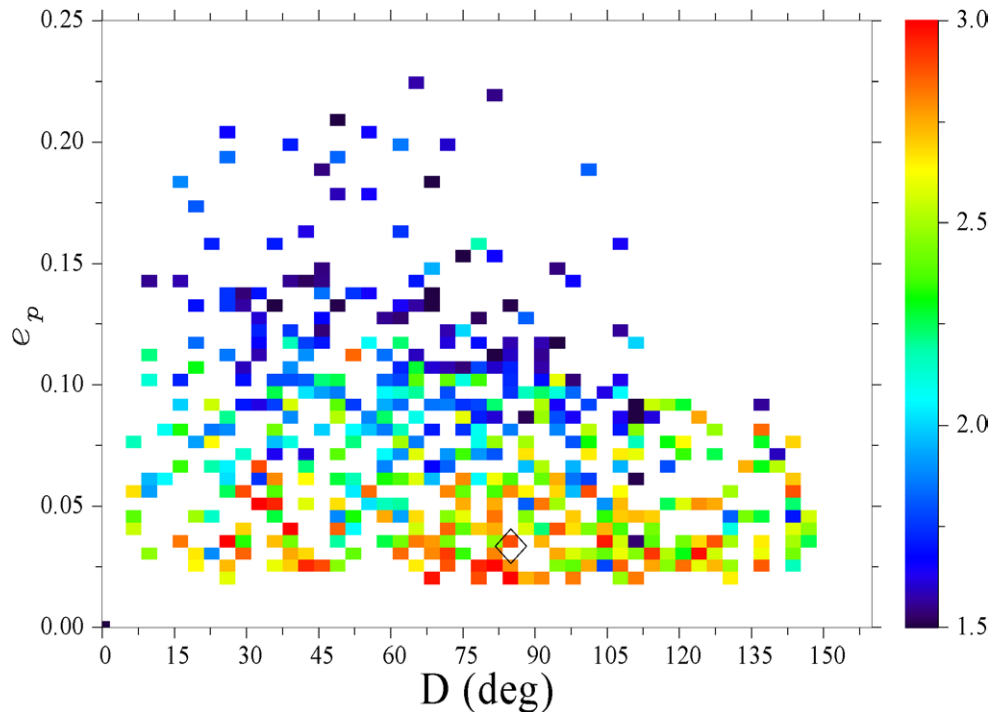


Fig. 2. Diffusion map in the  $D, e_p$  plane for proper inclinations in the interval  $15.0^\circ \pm 2.5^\circ$ .

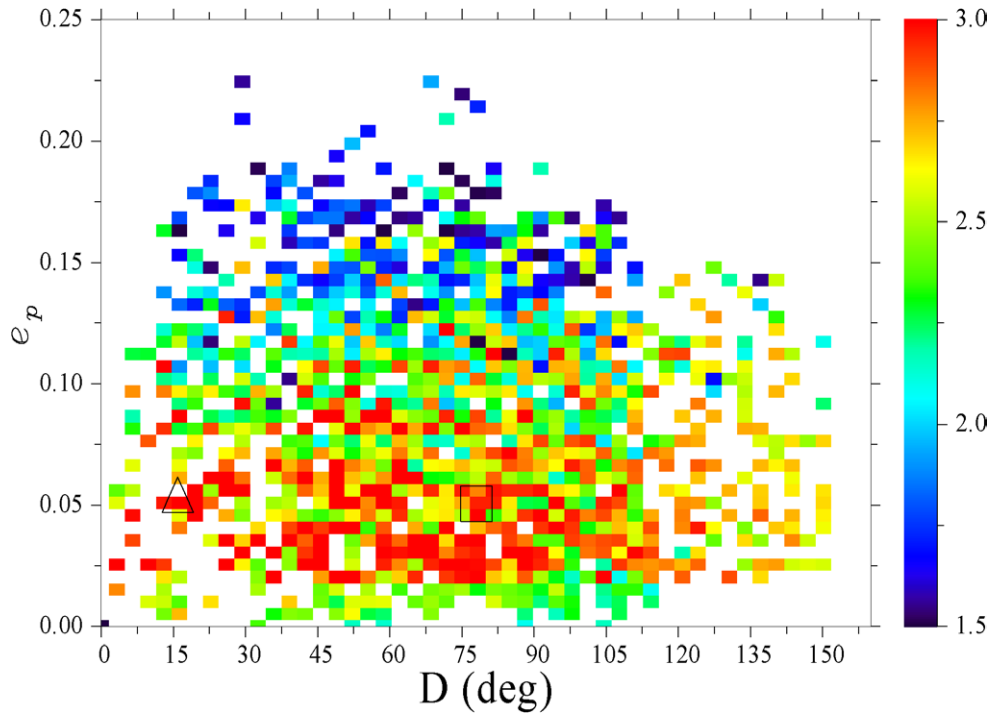


Fig. 3. Diffusion map in the  $D, e_p$  plane for proper inclinations in the interval  $20.0^\circ \pm 2.5^\circ$ .

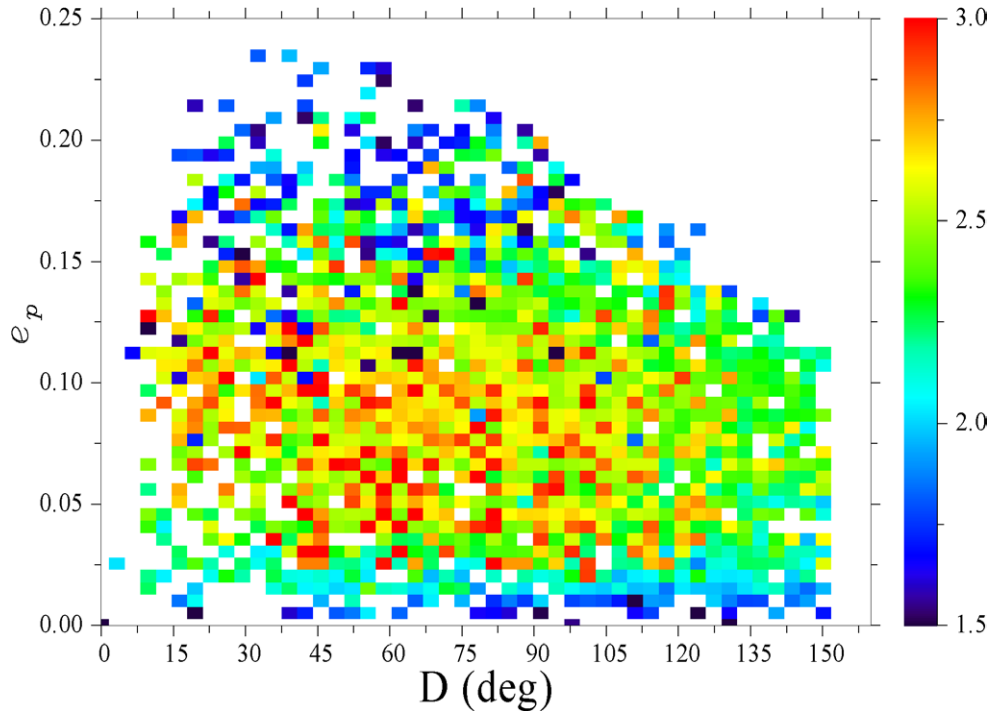


Fig. 4. Diffusion map in the  $D, e_p$  plane for proper inclinations in the interval  $25.0^\circ \pm 2.5^\circ$ .

perform a conventional fit of the frequencies as a function of  $e_p$ ,  $i_p$ , and  $D$ . We compare both  $g$  and  $s$  with the fundamental frequencies of the Solar System and thus we can map the location of secular resonances and identify those responsible for chaotic motion and fast instability. Mikkola and Innanen (1994) and Tabachnik and Evans (1999, 2000) guessed that

some secular resonances, like the  $\nu_5$ , the  $\nu_3$  and some higher order resonances, possibly destabilize Mars Trojans depending on their inclination. However, some of the critical arguments which they assume to cause secular perturbations do not fully comply with the D'Alembert rules. As an example, the resonance with argument  $2\dot{\omega} + \dot{\Omega} - g_5$  (Tabachnik and

Evans, 2000) has neither the sum of the coefficients equal to zero nor an even number of nodal frequencies. For this reason, we do not include this and a few other presumed secular resonances in our analysis.

The secular system of Mars Trojans is defined by the following equations:

$$g = 17.886 - 0.505x^2 - 16.050y^2 - 0.018z^2 + 0.562x^2y^2 - 0.127x^2z^2 + 0.382y^2z^2 + 0.469x^4 - 5.637y^4 - 0.044z^4, \quad (1)$$

$$s = -18.143 - 1.106x^2 + 8.659y^2 + 0.025z^2 - 0.190x^2y^2 - 0.006x^2z^2 - 0.118y^2z^2 + 0.096x^4 - 2.510y^4 - 0.001z^4, \quad (2)$$

$$f_l = 1047.401 - 28.301x^2 - 164.910y^2 - 114.261z^2 + 15.673x^2y^2 + 22.449x^2z^2 + 68.018y^2z^2 + 3.647x^4 + 8.329y^4 - 8.7903z^4. \quad (3)$$

The proper elements have been rescaled, according to Milani (1994), in the following way:

$$x = \frac{e_p}{0.15}, \quad y = \frac{\sin I_p}{0.6}, \quad z = \frac{da}{0.001 \text{ AU}}. \quad (4)$$

The amplitude of the semimajor axis oscillation  $da$  is related to the proper libration amplitude  $D$  through the formula  $D = da/0.0014992$  derived from the analytical theory of Erdi (Erdi, 1988). All the frequencies are expressed in arcsec/year. The relative error in each coefficient is less than 1%. The libration frequency computed from the above equation for an average value of  $e_p$  and  $D$ , qualitatively agree with the analytical prediction of Eq. (8) in Tabachnik and Evans (2000) and with Eq. (4) of Erdi (1988).

In Fig. 5 we show the location in the  $[e_p, i_p]$  plane of the principal secular frequencies that perturb the stability of Mars Trojans. There are several features in Fig. 1 that can be interpreted by looking at Fig. 5. Note that the secular resonances  $\nu_3, \nu_4, \nu_{13}, \nu_{14}$  related to the respective frequencies  $g_3, g_4, s_3, s_4$ , and the secular resonances related to Laskar's frequencies Lask<sub>4</sub>, Lask<sub>5</sub> and Lask<sub>6</sub> ( $j = 4, 5, 6$  in Table 9 of Laskar, 1988), generate instability at low inclinations. In particular, the resonance  $\nu_{14}$  corresponds to the lower limit of the stable region around  $i_p \sim 20^\circ$ . A comparison with Fig. 1 indicates that also the  $\nu_5$  resonance affects the stability around  $i_p \sim 28^\circ$ – $30^\circ$  causing a depletion of Trojan orbits in this inclination stripe for almost any value of proper eccentricity. For higher inclinations, Eqs. (1)–(2) predict a progressive slowing down of the perihelion argument until the frequency approaches zero. In Fig. 5, the line representing  $\dot{\omega} = 0$  is located at  $i_p \sim 50^\circ$ . It is marked by the label 'Kozai', presuming that orbits lying along this line are in a Kozai resonance. However, the width of the Kozai resonance extends down to lower values of  $i_p$ . Orbits within the stripe  $35^\circ < i_p < 45^\circ$  appear to be influenced by resonance overlapping. Fig. 7 illustrates a case with  $i_p = 42.7^\circ$  apparently dominated by the Kozai resonance. It is rapidly ejected out

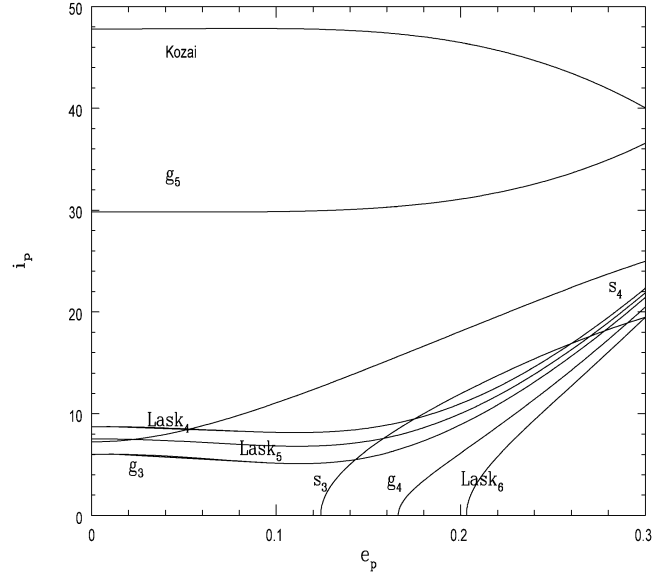


Fig. 5. Location of the major secular resonances in the  $e_p, i_p$  plane. The frequencies  $g_3, g_4, s_3, s_4$  are related to the respective secular resonances  $\nu_3, \nu_4, \nu_{13}, \nu_{14}$ . The lines labeled Lask<sub>4</sub>, Lask<sub>5</sub>, and Lask<sub>6</sub> are resonances with secular frequencies found in the power spectrum of Mars by Laskar (1988) in his Table 9 ( $f_{\text{Lask}_4} = 16.83285$  arcsec/yr,  $f_{\text{Lask}_5} = 17.10507$  arcsec/yr,  $f_{\text{Lask}_6} = 18.46529$  arcsec/yr). The line labeled 'Kozai' marks the transition from positive circulation to negative circulation of the perihelion argument, where a Kozai resonance may occur.

of the Trojan region and, once escaped, it is trapped in the Kozai resonance. The case shown in Fig. 6 with  $i_p = 39.3^\circ$  appears to belong to the Trojan resonance but the body enters and exits the Kozai resonance until it is finally destabilized after 9 Myr. In both cases, the eccentricity and inclination are oscillating in antiphase showing the influence of the perturbing term of the Kozai resonance. Trojan type orbits with  $i_p > 35^\circ$  cannot survive because of the increasing strength of the Kozai resonance.

#### 4. Timescales for slow and fast diffusion

Orbits in the region of high stability outlined in Section 2.2 with the FMA method, have slow diffusion speeds. Can we translate the diffusion speed of a Trojan orbit into survival time before leaving the Trojan region? A way to 'tune' the diffusion speed is to perform long-term numerical integrations of sample orbits over the Solar System age. By comparing the number of bodies that survive with those that escape we can estimate the half-life associated to the slowest diffusion rate, in other words we evaluate the average timescale for the chaotic wandering before escape out of the Trojan region.

We selected 20 orbits within the 'red' slow diffusion region with values of  $\sigma \geq 3$  thus possibly stable over a long timescale, and 20 highly chaotic orbits with  $\sigma \leq 1.5$ . We integrated their orbits over 4.5 Gyr under the gravitational perturbations of eight planets, from Mercury to Neptune. 12 of the 20 bodies residing in the stable region are still Mars

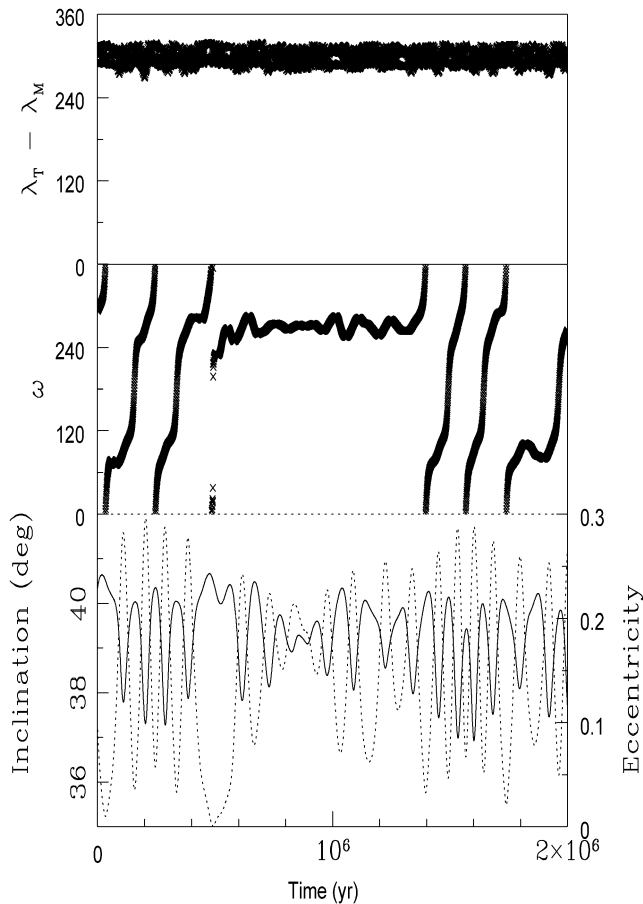


Fig. 6. The inclination, eccentricity, perihelion argument  $\omega$ , and critical argument  $\lambda$ , are plotted vs time for a representative Mars Trojan close to the Kozai resonance. The perihelion argument librates around  $270^\circ$ .

Trojans after 4.5 Gyr and their decay can be approximated with an exponential curve having a half-life of about 6 Gyr. All the 20 bodies with  $\sigma \leq 1.5$  escape within 60 Myr and their half-life is only 20 Myr. These simulations give an idea of the residence times associated with the slow (and fast) diffusion orbits.

We calculated also the other available indicator of chaos, the Lyapunov exponent, for the same 20 bodies by using the ORBIT9 integrator described in Milani and Nobili (1988), available at the site <http://tycho.dm.unipi.it/~planet/software.html>. The numerical code solves both the equation of motion and the corresponding variational equation that is the linearized differential equation of the relative motion between two nearby orbits. An estimate of the maximal Lyapunov characteristic exponent (LCE) that characterizes the rate of exponential divergence between two orbits, is computed as the coefficient of a least squares linear fit to the function  $\gamma(t) = \log(D(t)/D(0))$ , where  $D(t)$  is the solution of the variational equation, and  $D(0)$  its initial value, a randomly chosen displacement value (Milani and Nobili, 1992; Milani, 1993). The variation vector is renormalized when it becomes too large. This method allows to detect a positive LCE over an integration time span that is between 6 and 7

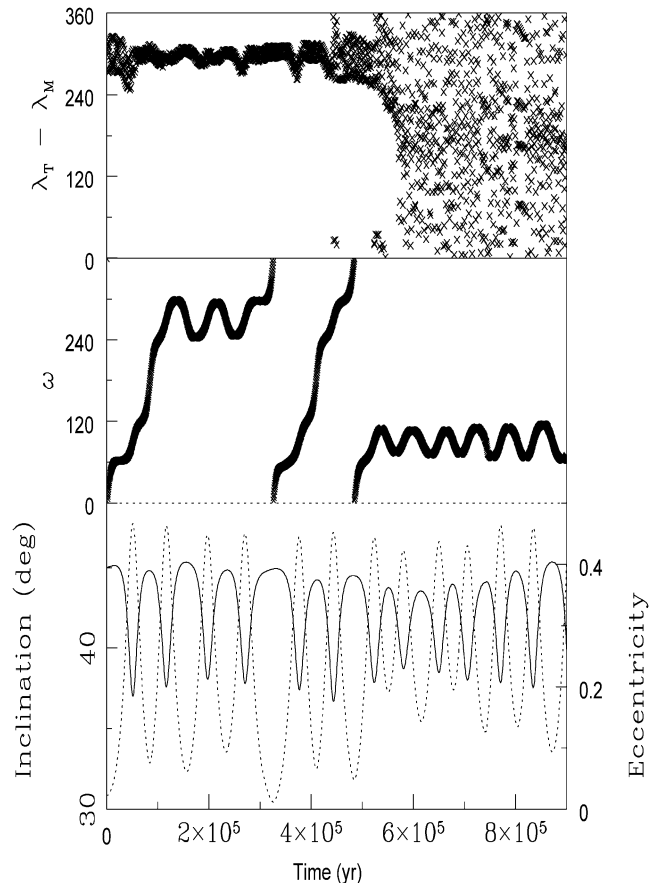


Fig. 7. Mars Trojan close to the border of the Kozai resonance. When entering the Kozai resonance the perihelion argument  $\omega$  starts to librate around  $90^\circ$  and the critical argument  $\lambda$  starts to circulate.

times the  $1/\text{LCE} = T_L$ , with  $T_L$  the Lyapunov time. We integrated the orbits of the 20 Mars Trojans for 50 Myr and we found that 16 bodies have an  $T_L$  lower than 5 Myr, a positive detection of chaos. The four remaining bodies are likely to be chaotic with an LCE of the order of a few  $10^{-8}$ . We did not continue the integration since the accumulation of the rounding-off error might yield to a non-reliable estimate of the LCE. The timestep used in our integration is small (2 days) to properly account for the orbit of Mercury (ORBIT9 is a multi-step integrator). The four bodies are anyway chaotic on the long term as shown from their evolution over 4.5 Gyr.

## 5. Instability in the slow diffusion region

The long-term integrations of the most stable orbits show that Mars Trojans are always chaotic. Orbits can be destabilized on timescales ranging from a few thousand of years to Gyrs. A non-negligible number of orbits has dynamical lifetimes exceeding the age of the Solar System. Their behavior is similar to that of the higher inclined Jupiter Trojans (Marzari et al., 2003a). How do Mars Trojans evolve while residing in the slow diffusion regions? The critical

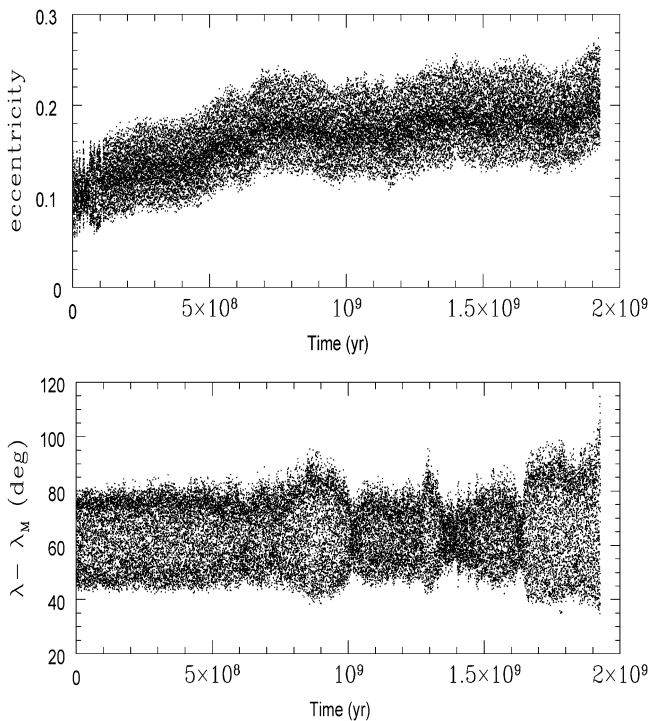


Fig. 8. Typical chaotic behavior of an unstable Trojan in the slow diffusion region. First, the eccentricity grows and it stabilizes at a large value. The critical argument  $\lambda$  shows chaotic variations until the body escapes from the Trojan region after an encounter with the planet.

parameters for stability are libration amplitude and eccentricity. Both parameters are responsible for close encounters with Mars. Fig. 8 shows the evolution of these parameters for one of the 20 slow diffusion Trojans which became unstable. The eccentricity gradually increases while the libration amplitude has large chaotic variations. After about 1.9 Gyr both the parameters are large enough for the asteroid to have a close encounter with the planet that destabilizes the orbit and eject the body out of the Trojan region. Fig. 9 shows the evolution of a case which remains a Mars Trojan for 4.5 Gyr. Like for the unstable case, the eccentricity increases while the libration amplitude remains almost constant. A burst of the libration amplitude occurs after 3.6 Gyr. Note that the ‘saturation’ eccentricity is higher in the unstable case, leading to a faster escape from the Trojan region. This burst is obviously not strong enough to destabilize the orbit. A subsequent stronger burst will possibly destabilize the orbit in the future. All orbits in the slow diffusion region show this behavior: the eccentricity steadily grows till a saturation value while chaotic bursts in the libration amplitude occur which lead to instability.

## 6. Dynamical lifetimes of the four known Trojans

What are the dynamical lifetimes of the four known Mars Trojans? As outlined above, they all reside in regions with low diffusion rate. In these regions, the dynamical half-life is of the order of the age of the Solar System.

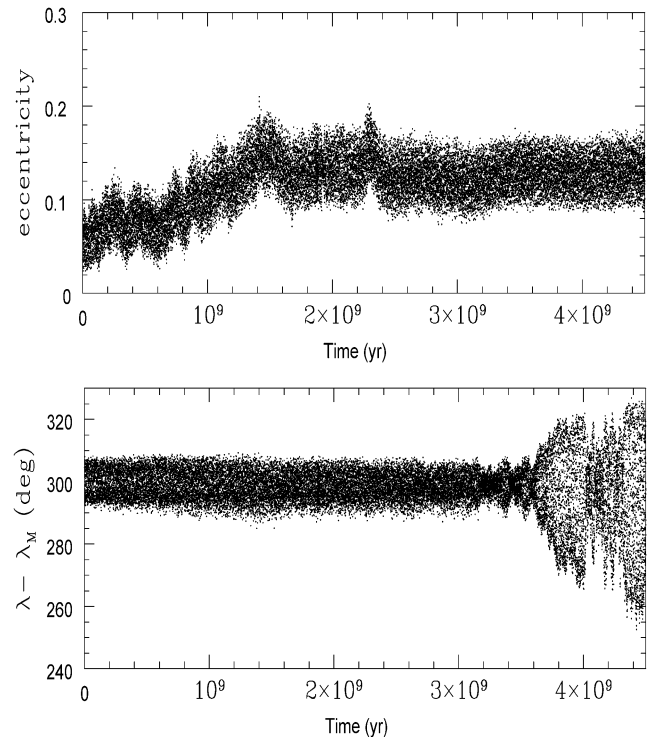


Fig. 9. Typical chaotic behavior of a long surviving Mars Trojan. The eccentricity grows at the beginning like for the unstable case shown in Fig. 8, even if it stabilizes near a lower value. The libration amplitude has a sudden burst at about 3.6 Gyr. Eccentricity and libration amplitude do not exceed threshold values for instability. This will possibly occur later.

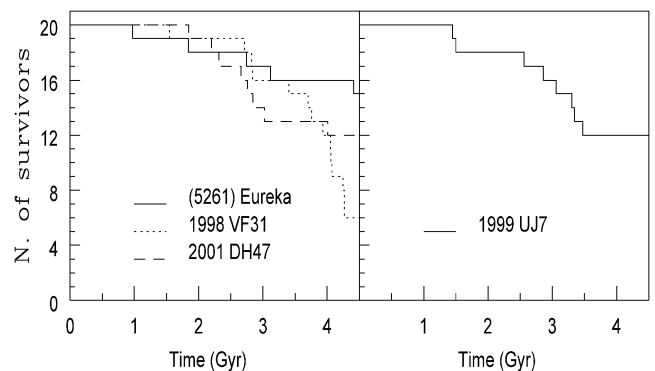


Fig. 10. Survival curves of the 20 clones of all known four Mars Trojans. 1999 UJ7 is the only L4 Trojans. Eureka has the longest half-life-time.

We integrated a sample of 20 clones for each Trojan. The orbits of the 20 clones of Eureka, 1998 VF31, and 1999 UJ7 were obtained by using their corresponding covariance matrix (<http://hamilton.dm.unipi.it/astdys>). This matrix can be obtained as a by-product of an orbit determination. For the clones of the other Trojan, where such a matrix is not presently available, we varied slightly its orbital elements. Osculating orbital elements of the four Trojans were taken from *Bowell’s Asteroid Orbital Elements Database* (<ftp.lowell.edu>).

Fig. 10 shows the survival times for the 20 clones of all four Trojans. Eureka appears to have the longest half-

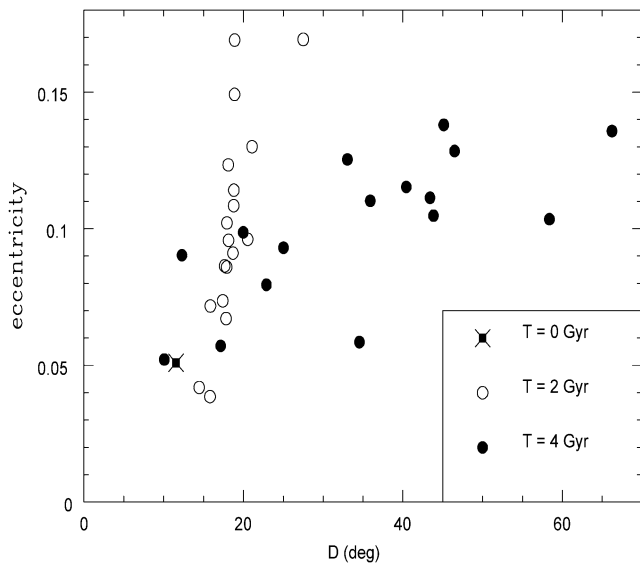


Fig. 11. Proper eccentricity vs proper libration amplitude  $D$  for 20 clones of Asteroid (5261) Eureka derived from its covariance matrix. The symbol X marks the location of the clones at  $t = 0$ . The empty circles show the spreading of the clones after 2 Gyr, while the filled circles correspond to the same clones after 4 Gyr.

lifetime largely exceeding the age of the Solar System followed by 1999 UJ7 and then by 2001 DH47. The half-lifetime of 1998 VF31 is shorter than 4.5 Gyr. This result is in accordance with the FMA analysis. All four Trojans reside in the ‘red’ region as shown in Fig. 1. Eureka resides deep in this region while 1998 VF31 is situated on the border of a ‘red’ island.

The destabilization of orbits is illustrated in Fig. 11 where we show at different times the proper elements of the Eureka clones. All orbits follow the same track: first, eccentricities increase and then libration amplitudes.

Taking into account the derived half-lifetimes, one cannot exclude that all four Mars Trojans are primordial residing in the Trojan region since a very early phase of the Solar System. Possible scenarios for their origin are discussed below.

## 7. The Yarkovsky effect

At this point, we have enough evidence to suggest that all the four known Mars Trojans survived over 4.5 Gyr. This is, however, only true in a purely gravitational model. As indicated above, the four Mars Trojans discovered so far are km-sized bodies (see Table 1). Their motion might, therefore, be affected by the Yarkovsky force. This is a thermal radiation force that causes a slow semimajor axis drift due to the re-emission of the absorbed solar radiation in the infrared (see Bottke et al. (2002) for a review). According to Nesvorný et al. (2002), a 1-km asteroid orbiting in the Main Belt at about 2.25 AU may migrate in semimajor axis of about 0.04 AU in 400 Myr. Mars Trojans orbit even closer to the Sun with a higher insolation. The mobility driven by the diurnal and seasonal Yarkovsky effect could, on the long term, destabi-

lize the Mars Trojans and throw them out of the resonance. This would mean that the known Mars Trojans did not originate in this region.

We, therefore, numerically integrated the orbits of the 20 most stable Mars Trojan orbits ( $\sigma \sim 3$ ) and of the clones of both (5261) Eureka and 1998 VF31 accounting for the Yarkovsky effect. For the 20 most stable orbits we performed simulations assuming different sizes for the bodies to find the threshold diameter for stability. For the (5261) Eureka and 1998 VF31 clones we used the estimated diameter (Rivkin et al., 2003) of the two asteroids. All the simulations were performed by using the package *swift-rmvs3*, modified by M. Broz to include the Yarkovsky effect (<http://sirrah.troja.mff.cuni.cz/mira/mp/>). In these simulations we have to define reasonable values for several parameters of the Yarkovsky force. The Mars Trojan obliquities are presently unknown and we adopted an intermediate value  $\epsilon = 45^\circ$ . The rotation period is not well defined from lightcurves and it could be in the 4.8–6.2 h range or longer, according to Rivkin et al. (2003). We adopted a value of 6 h. The two Mars Trojans have spectra consistent with the Sr class (Rivkin et al., 2003) and the only Sr asteroid observed with IRAS, (984) Gretia, has an albedo of about 0.42, that we used in our simulations. For the other parameters characterizing the Yarkovsky force we followed Nesvorný et al. (2002) and adopted a bulk density of  $2.5 \text{ g/cm}^3$ , a surface density of  $1.5 \text{ g/cm}^3$ , a surface conductivity  $K = 0.001 \text{ W/(mK)}$ , and an emissivity of 0.9. With this choice of parameters, a critical question is the presence of regolith on the surface of the asteroids which influences both the values of surface density and conductivity  $K$ . In our numerical experiments we also neglect spin axis reorientation that, according to Farinella and Vokrouhlický (1999), should occur every  $\tau_r = 10.6\sqrt{D}$  in Myr, where  $D$  is the diameter in meters. For a 1 km-sized body like Eureka or 1998 VF31,  $\tau_r$  would be about 330 Myr. However, Mars Trojans are far from the inner border of the asteroid belt and a very low flux of potential projectiles is expected, significantly increasing the time required for a reorienting impact.

In order to estimate the threshold size below which the Yarkovsky effect destabilizes Trojan orbits, we show in Fig. 12 the survival curves of the 20 most stable Mars Trojan orbits for different values of their diameter. The figure indicates that the stability of Mars Trojans with a diameter of about 1 km like (5261) Eureka and 1998 VF31, is not significantly affected by the Yarkovsky effect. However, for diameters  $\sim 1\text{--}5 \text{ m}$  there is a remarkable reduction in the number of surviving bodies. This indicates that primordial Trojans with diameters less than a few meters possibly did not survive until present. The values for the diameters in Fig. 12 are, of course, only approximative since we did not vary all possible parameters described above. If observational surveys detect Mars Trojans in the meter-size range, they are presumably temporary bodies in this region.

The simulations for the (5261) Eureka and 1998 VF31 clones with the Yarkovsky force show that their escape rate

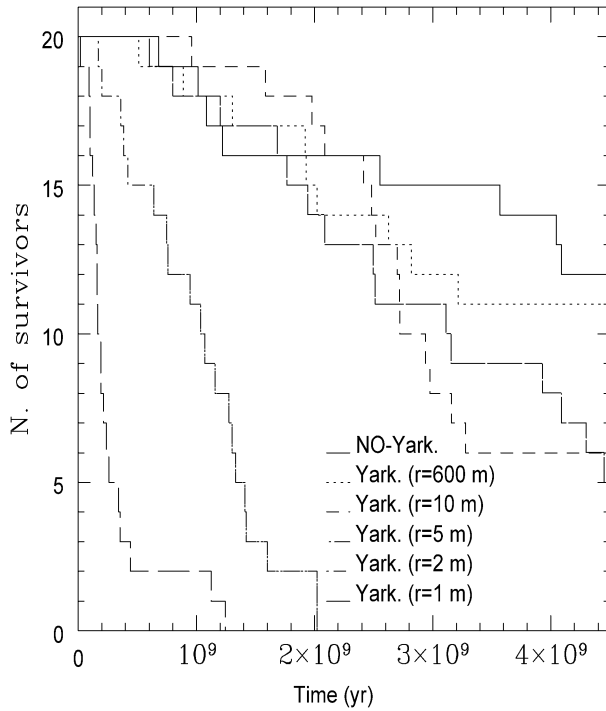


Fig. 12. Survival curve for the 20 most stable Mars Trojans ( $\sigma \sim 3$ ) taking into account the Yarkovsky effect for two different asteroid sizes.

is not significantly changed. Since for Eureka and 1998 VF31 the dynamical lifetimes were not affected, we did not investigate the Yarkovsky effect on the two remaining Trojans.

## 8. Origin

According to the previous results, all four Mars Trojans may reside in the Trojan region since early times of the Solar System. Was it possible for Mars to trap them during its formation or just right after?

Various mechanisms have been proposed so far to explain the capture in Trojan-type orbits during the early phases of the Solar System evolution. The most popular mechanisms are related to the mass growth of the planet, to the collisional diffusion of planetesimals, and to gas drag friction (see Marzari et al., (2003a, 2003b) for a detailed discussion). We can exclude mass growth of the planet which is an efficient mechanism when the planet has a period of fast growth, as Jupiter (or Saturn) does during the gas infall, while it appears unrealistic for a terrestrial planet like Mars. A dissipative force is a good candidate. However, the gas drag was possibly too strong in the inner Solar System and the nebular gas possibly dissipated while planetary accretion was still going on.

Could bodies migrate into the Trojan region due to the Yarkovsky force? We numerically integrated the orbits of numerous small bodies starting in the proximity of Mars. All bodies had numerous close encounters with Mars before

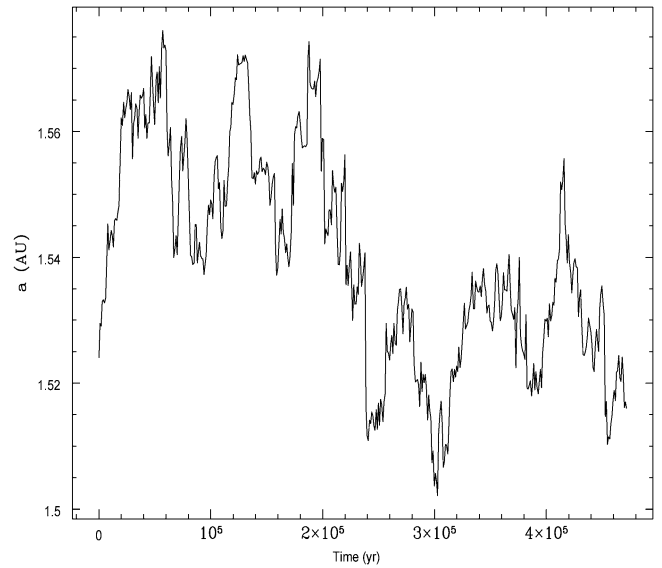


Fig. 13. Simulated migration of a proto-Mars in the early phases of its formation under the perturbations of nearby planetary embryos.

they had a chance to be driven into the safe Trojan region by the Yarkovsky force. In the simulations we did not find any body trapped as a Mars Trojan. Collisional diffusion appears to be feasible, but it is by far the less efficient capture mechanism due to the narrowness of the libration regions surrounding the Lagrange points L4 and L5 of Mars.

An appealing mechanism has been proposed to us by A. Morbidelli (private communication). In the final stage of terrestrial planet formation, the orbit of proto-Mars was possibly perturbed by lunar-sized bodies, the remains of the planetary accretion process. These bodies collide finally with either of the terrestrial planets or they will be ejected out of the Solar System at the end of the ‘giant impact’ phase. A major consequence of close encounters, or even impacts, between proto-Mars and these lunar-sized bodies is a chaotic wandering of the proto-planet in semimajor axis. During each change of semimajor axis, the regions surrounding both L4 and L5 move with the planet to a new location possibly populated by small planetesimals, leftover of the runaway growth of planetary embryos. A fraction of the local planetesimals may be trapped within the region of tadpole orbits and become Mars Trojans. Such planetesimals might have inclinations between  $15^\circ$  and  $30^\circ$  which is necessary to become a stable Mars Trojan. In Fig. 13 we show an example of the chaotic evolution of the orbit of a Mars-size planet perturbed by 40 Moon-sized embryos distributed within  $\pm 0.4$  AU from the planet’s orbit with small initial eccentricities ( $e < 0.001$ ). The orbits of all the bodies were integrated within a full N-body problem over  $5 \times 10^5$  yr with the Mercury code (Chambers and Migliorini, 1997). This simulation is only indicative but it shows that the planet may indeed change its orbit shifting the position of the Lagrangian points to new regions of the planetesimal disk. A critical question is whether the planetesimals, once trapped in tadpole orbits, would survive as Trojans

during the following wandering of the planet in semimajor axis. Fleming and Hamilton (2000) showed that a smooth or adiabatic change in semimajor axis of the planet does not destabilize Trojans. Of course, in the case of chaotic migration induced by close encounters, the change in semimajor axis can be abrupt violating the necessity of an adiabatic change. Moreover, drifting through mean motion resonances with other planets might have induced strong instabilities on a putative Mars Trojan population (Michtchenko and Ferraz-Mello, 2001). During its chaotic wandering, Mars may have trapped and lost Trojans. The presently observed Trojans may have been captured during one of the last close encounters with a lunar-sized body.

As outlined in Section 1, the spectral classes of the known Trojans are quite surprising (see Table 1). While the spectral class of 2001 DH47 is considered to be in accordance with those of near main belt asteroids, the spectral classes of Eureka and 1998 VF31 are unusual. Their mineralogy suggests that both bodies were part of a larger, possibly differentiated parent body (Rivkin et al., 2003). Since both bodies are protected against migration due to the Yarkovsky force, they may be the only remnant of planetesimals that formed in the terrestrial planetary region. The spectral class of the only L4 Trojan, 1999 UJ7, has not yet been determined due to its faintness.

## 9. Discussion and conclusions

We investigated the stability of the Mars Trojan region by using the Frequency Map Analysis of Laskar (Laskar et al., 1992; Laskar 1993a, 1993b). This method yields firstly a measure for the diffusion speed in the phase space of proper elements and, secondly, the proper frequencies of the system. Diffusion is comparatively slow for orbital inclinations between about  $15^\circ$  and  $30^\circ$ . Outside of this range, diffusion is fast and instability sets on within some millions of years. The proper frequencies enable to build a secular theory for Mars Trojan orbits that allows to understand the unstable regions. Below  $15^\circ$  are several secular resonances, in particular the  $\nu_3$ ,  $\nu_4$ ,  $\nu_{13}$ ,  $\nu_{14}$  resonances, which excite orbital eccentricities. For large inclinations, the secular resonance  $\nu_5$  clears a small region around  $30^\circ$  while the Kozai resonance rapidly removes bodies for inclinations larger than  $35^\circ$ .

Orbits with inclinations in the range  $15^\circ$  to  $30^\circ$  are chaotic. Nevertheless, a non-negligible number of orbits remains stable over the age of the Solar System. The three L5 Trojans (5261) Eureka, 1998 VF31, 2001 DH47, and the only L4 Trojan 1999 UJ7 all reside in the most stable region. All four bodies may reside in the Trojan region since early times of the Solar System. It cannot be guaranteed since when integrating clouds of clones, a few clones always become unstable before 4.5 Gyrs. At least half of the clones of each cloud, however, do survive.

The four known Trojans are km-sized bodies. Hence, their orbits are, a priori, affected by the Yarkovsky force.

However, according to our results, the Trojan resonance locking prevails against the Yarkovsky force for bodies larger than about 1–5 m. Mars Trojans may be primordial bodies, possibly the only remnants of planetesimals formed in the terrestrial planet region.

The mechanism by which Mars Trojans were captured is still unknown. An appealing scenario predicts that the Mars trapped small bodies, possibly planetesimals, during its chaotic wandering due to close encounters with planetary embryos.

## References

- Bottke Jr., W.F., Vokrouhlicky, D., Rubincam, D.P., Broz, M., 2002. The effect of Yarkovsky thermal forces on the dynamical evolution of asteroids and meteoroids. In: Bottke Jr., W.F., Cellino, A., Paolicchi, P., Binzel, R.P. (Eds.), *Asteroids III*. Univ. Arizona Press, Tucson, pp. 395–408.
- Brasser, R., Lehto, H.J., 2002. The role of secular resonances on Trojans of the terrestrial planets. *Mon. Not. R. Astron. Soc.* 334, 241–247.
- Brasser, R., Mikkola, S., Huang, T.-Y., Wiegert, P., Innanen, K., 2004. Long-term evolution of the Neptune Trojan 2001 QR322. *Mon. Not. R. Astron. Soc.* 347, 833–836.
- Carpino, M., Milani, A., Nobili, A.M., 1987. Long-term numerical integrations and synthetic theories for the motion of the outer planets. *Astron. Astrophys.* 181, 182–194.
- Chambers, J.E., Migliorini, F., 1997. Mercury—a new software package for orbital integrations. *Bull. Am. Astron. Soc.* 29, 1024.
- Erdi, B., 1988. Long periodic perturbations of Trojan asteroids. *Celest. Mech.* 43, 303–308.
- Everhart, E., 1985. Dynamics of comets: their origin and evolution. In: *Astrophys. Space. Sci. L*, vol. 115. IAU Colloq. 83, p. 185.
- Farinella, P., Vokrouhlicky, D., 1999. Semimajor axis mobility of asteroidal fragments. *Science* 283, 1507–1510.
- Fleming, H.J., Hamilton, D.P., 2000. On the origin of the Trojan asteroids: effects of Jupiter's mass accretion and radial migration. *Icarus* 148, 479–493.
- Laskar, J., 1988. Secular evolution of the Solar System over 10 million years. *Astron. Astrophys.* 198, 341–362.
- Laskar, J., 1993a. Frequency analysis for multi-dimensional systems: global dynamics and diffusion. *Physica D* 67, 257–281.
- Laskar, J., 1993b. Frequency analysis of a dynamical system. *Celest. Mech. Dynam. Astron.* 56, 191–196.
- Laskar, J., Froeschlè, C., Celletti, A., 1992. The measure of chaos by the numerical analysis of the fundamental frequencies: application to the standard mapping. *Physica D* 56, 253–269.
- Levison, H., Duncan, M.J., 1994. The long-term dynamical behavior of short-period comets. *Icarus* 108, 18–36.
- Marzari, F., Scholl, H., 1998. Capture of Trojans by a growing proto-Jupiter. *Icarus* 131, 41–51.
- Marzari, F., Tricarico, P., Scholl, H., 2002. Saturn Trojans: stability regions in the phase space. *Astrophys. J.* 579, 905–913.
- Marzari, F., Tricarico, P., Scholl, H., 2003a. Stability of Jupiter Trojans investigated using frequency map analysis: the MATROS project. *Mon. Not. R. Astron. Soc.* 345, 1091.
- Marzari, F., Tricarico, P., Scholl, H., 2003b. The MATROS project: stability of Uranus and Neptune Trojans. The case of 2001 QR322. *Astron. Astrophys.* 410, 725–734.
- Melita, M.D., Brunini, A., 2001. A possible long-lived asteroid population at the equilateral Lagrangian points of Saturn. *Mon. Not. R. Astron. Soc.* 322, L17–L21.
- Milani, A., 1993. The Trojan asteroid belt: proper elements, stability, chaos and families. *Celest. Mech. Dynam. Astron.* 57, 59.
- Milani, A., 1994. The dynamics of Trojan asteroids. In: Milani, A., Di Martino, M., Cellino, A. (Eds.), *Asteroids, Comets, Meteors*, p. 159.

- Milani, A., Nobili, A., 1988. Integration error over a very long timespan. *Celest. Mech. Dynam. Astron.* 43, 1.
- Milani, A., Nobili, A., 1992. An example of stable chaos in the Solar System. *Nature* 357, 569.
- Millis, R.L., Buie, M.W., Wasserman, L.H., Elliot, J.L., Kern, S.D., Wagner, R.M., 2002. The Deep Ecliptic Survey: a search for Kuiper belt objects and centaurs: I. Description of methods and initial results. *Astron. J.* 123, 2083–2109.
- Mikkola, S., Innanen, K., 1994. On the stability of martian Trojans. *Astron. J.* 107, 1879–1884.
- Michtchenko, T.A., Ferraz-Mello, S., 2001. Resonant structure of the outer Solar System in the neighborhood of the planets. *Astron. J.* 122, 474–481.
- Morbidelli, A., Levison, H.F., Tsiganis, K., Gomes, R., 2004. The capture of Jupiter Trojans during the passage of Jupiter and Saturn through their mutual 1:2 mean motion resonance. In: AAS DPS Meeting 36. Abstract 40.03.
- Murray, C.D., 1994. Dynamical effects of drag in the circular restricted three-body problem: 1. Location and stability of the Lagrangian equilibrium points. *Icarus* 112, 465–484.
- Nesvorný, D., Dones, L., 2002. How long-lived are the hypothetical Trojan populations of Saturn, Uranus, and Neptune? *Icarus* 160, 271–288.
- Nesvorný, D., Ferraz-Mello, S., 1997. On the asteroidal population of the first-order jovian resonances. *Icarus* 130, 247–258.
- Nesvorný, D., Morbidelli, A., Vokrouhlický, D., Bottke, W.F., Broz, M., 2002. The Flora family: a case of the dynamically dispersed collisional swarm? *Icarus* 157, 155–172.
- Peale, S.J., 1993. The effect of the nebula on the Trojan precursors. *Icarus* 106, 308–322.
- Rivkin, A.S., Binzel, R.P., Howee, E.S., Bus, S.J., Grier, J.A., 2003. Spectroscopy and photometry of Mars Trojans. *Icarus* 165, 349–354.
- Šidlichovský, M., Nesvorný, D., 1997. Frequency modified Fourier transform and its application to asteroids. *Celest. Mech. Dynam. Astron.* 65, 137.
- Tabachnik, K.S., Evans, N.W., 1999. Cartography for martian Trojans. *Astrophys. J.* 517, L63–L66.
- Tabachnik, S.A., Evans, N.W., 2000. Asteroids in the inner Solar System: I. Existence. *Mon. Not. R. Astron. Soc.* 319, 63–79.
- Wisdom, J., Holman, M., 1991. Symplectic maps for the  $n$ -body problem. *Astron. J.* 102, 1528–1538.

### Further reading

- Marzari, F., Farinella, P., Davis, D.R., Scholl, H., Campo Bagatin, A., 1997. Collisional evolution of Trojan asteroids. *Icarus* 125, 39–49.